ELSEVIER

Journal of Hazardous Materials B138 (2006) 133–141

Journal of Hazardous Materials

www.elsevier.com/locate/jhazmat

The removal of anionic dyes from aqueous solutions in the presence of anionic surfactant using aminopropylsilica—A kinetic study

Antonio R. Cestari *, Eunice F.S. Vieira, Gláucia S. Vieira, Luis E. Almeida

Laboratory of Materials and Calorimetry, Departamento de Química/CCET, Universidade Federal de Sergipe, CEP 49100-000 São Cristóvão, Sergipe, Brazil

Received 22 March 2006; received in revised form 11 May 2006; accepted 16 May 2006
Available online 22 May 2006

Abstract

In this study, the aminopropyl-silica (Sil-NH_2) was used to adsorb a yellow- and a red-dye from aqueous solutions at pH 4.0. New data concerning the influence of the anionic surfactant SDS on the adsorption data was obtained. All interactions occurred below the cmc values of the Sil-NH_2/anionic dyes aggregates. A rise of temperature accelerates the mass transfer of the red-dye into the Sil-NH_2 surface, while the yellow-dye adsorption decreased. The presence of SDS increased the adsorption quantities in relation to the temperature increasing. The exception is observed for the yellow-dye adsorption at 55 °C. So, it is suggested that the chemical structure of the dye, as well as the presence and position of its sulfonate groups are important factors that affect the anionic dye/SDS aggregations and the adsorption quantities.

The solid-phase interactions of dyes data present good fittings to the Avrami kinetic model, where from two to four kinetic regions were found, taking into account the variations of the contact time and temperature. The presence of several values of Avrami constants, namely k_{Av} and n, has been attributed to the occupation of both the surface and the internal adsorption sites of the aminopropyl-silica.

Keywords: Silica gel; Dyes adsorption; Anionic surfactants; Kinetic modelings

1. Introduction

The treatment of wastewater has long been a major concern in the environmental field. The total dye consumption of the textile industry worldwide is in excess of 10^7 kg per year, and an estimated 90% of this ends up on fabrics. So, approximately 1 million kg per year of dyes are discharged into water streams by the textile industry. Dye producers and users are interested in stability and fastness, and consequently, are producing dyestuffs, which are more difficult to degrade after use [1]. Unless properly treated, the dyes present in wastewaters can affect photosynthesis activity due to reduced light penetration and may also be toxic to certain forms of aquatic life.

Adsorption has been shown to be the most promising option for non-degradable dyes for the removal from aqueous streams. Activated carbons are the most common adsorbents for this process due its effectiveness, versatility, and good capacity for the adsorption of dyes and other organic molecules. However, it suffers from a number of disadvantages, mainly its high cost on large-scale uses [2–4].

Functionalized mesoporous oxides have been used as effective adsorbents [5] because of their high surface area and the functionalized pore channels of large diameter. Their high surface areas allow the binding of a large number of surface groups and the functionalized pore channels of large diameter allow an easy reaction with adsorbates in aqueous phase. Among a great variety of supporting materials, silica gel is of particular interest due to its stability, possible reuse, and relative rapidity in reaching equilibrium, high mechanical resistance, and high surface area. Silicas are extensively modifiable materials [6]. The modification results in products, which carry on their surface new functional groups, capable of interacting with various organic compounds [7]. For example, application of aminosilane-silica can be found in HPLC retention of poly-aromatic-hydrocarbons [8], immobilization of electrochemical actives Ru complexes [9] and capillary electrochromatographic separations of tetracycline derivatives [10]. Aminosilane-silica have also been used with increasing frequency as coupling agents in pigment or organic dye systems [11,12].

* Corresponding author. Tel.: +55 7932126656; fax: +55 7932126651.
E-mail address: cestari@ufs.br (A.R. Cestari).

0304-3894/$ – see front matter © 2006 Elsevier B.V. All rights reserved.
doi:10.1016/j.jhazmat.2006.05.046

The sorption of dyes onto sorbents is influenced dramatically by the presence of surfactants. They, especially the anionic ones, are produced and utilized in huge amounts in various industrial branches and emitted into wastewaters [13]. They are, therefore, almost ubiquitous in the environment now. However, almost nothing is known about the role of the presence of the anionic surfactants in the kinetic modelings of the adsorption of dyes at solid/solution interface. For this reason, some new aspects concerning to the kinetic modeling of the removal of anionic dyes using aminosilane-silica, in relation to the presence of an anionic surfactant, the chemical structures of the dyes and adsorption temperature, are presented in this work.

2. Materials and methods

2.1. Materials

Silica gel 60 (Merck), for column chromatography, presenting particle size and average pore size of 60–230 mesh and 60 Å, respectively, was used in the present work. It was previously heated at 150 °C for 12 h in a vacuum line. All chemicals used were reagent grade. The silylating agent 3-(trimethoxysilyl)propylamine, 99% purity (hereafter called as apts for simplicity), from Aldrich, and dodecylbenzene sulfonic acid, sodium salt, 97% purity (hereafter called as SDS for simplicity), from Sigma, were used without purification.

The dyes, commercially available as Reactive Yellow GR (A, hereafter called as yellow-dye) and Reactive Red RB (B, hereafter called as red-dye) were free gifts from The Santista Textiles Industries (Sergipe/Brazil), which were provided by The Dystar Dyes Company and used without purification. Fig. 1 shows the chemical structures of the dyes.

2.2. Synthesis of the aminopropyl-silica

The synthesis of the aminopropyl-silica followed the procedure described elsewhere [14]. Briefly, about 50 g of activated silica was immersed in 200 mL of dry xylene and 20 mL of apts was added. The suspension was mechanically stirred under solvent reflux for 48 h. The resulting alkoxysilane-modified silica gel (hereafter called as Sil-NH_2 for simplicity), was filtered, washed with xylene, ethanol and ethylic ether, and conditioned in a dark air-free flask, in order to prevent interactions between the immobilized amino groups and atmospheric CO_2 [15].

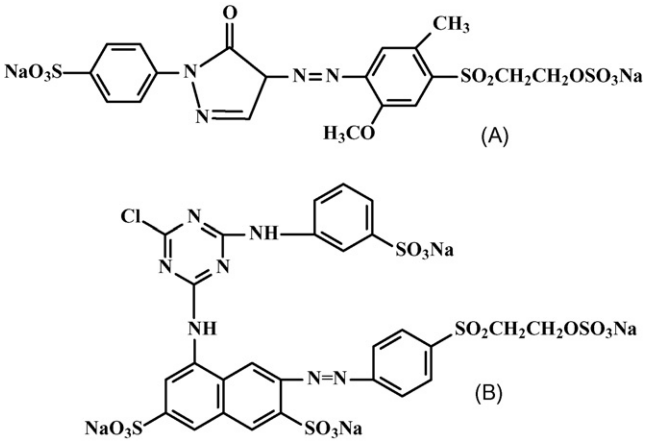

Fig. 1. Chemical structures of the yellow-dye (A) and red-dye (B).

2.3. Characterization of the silicas

The thermogravimetric analyses (TG and DTG) were made using about 10 mg of the unmodified silica and Sil-NH_2, in separated runs, under nitrogen atmosphere at 10 °C min^{-1}, from 25 to 800 °C, in a SDT 2960 thermoanalyser, from TA Instruments. The amount of nitrogen was made by the Kjeldhal method and checked by TG [16]. The surface areas determinations were made in a FlowSorb 2300 surface area analyser from Micromeritics, from N_2 adsorptions at −195 °C using the BET procedure [17].

2.4. Determination of the cmc of the systems surfactant–dyes

The critical micelle concentration (cmc) values for each surfactant–dye system in sodium ftalate/NaOH buffered solutions at pH 4.0 were measured conductometrically [18] by using a Micronal model conductivimeter, having an electrode with cell constant of 0.93 cm^{-1}. A pH 4.0 SDS solution at 400 mg L^{-1} were progressively diluted in 100 mL of the initial dye solution at 100 mg L^{-1}, and the specific conductivities values at 25 °C were measured. The cmc values for each surfactant–dye system were determined by plotting the values of the specific conductivities against the respective surfactant concentrations in solution. Blank tests using pure water, the pH 4.0 buffered solutions without dye were also performed.

2.5. Kinetics of the dyes removal

Sodium ftalate/NaOH buffered solutions at pH 4.0 were used as solvent, because the adsorption of anionic dyes is maximized at this pH value [19]. In addition, the silica-attached aminopropyl molecule can be affected, even removed from the silica surface, when very acidic solutions (pH less than 3.5) are used [20]. The adsorption kinetic experiments were performed by batch procedures, from 25 to 55 ± 0.1 °C, using dyes aqueous solutions at 23.0 mg L^{-1}. This initial dyes concentration value was chosen to verify the performance of the Sil-NH_2 to remove dyes when very diluted dyes solutions are used. In each adsorption experiment, 50 mL of the dye solution was added to 100 mg of the Sil-NH_2 in a 150 mL polyethylene flask, and stirred continuously at a determined temperature, as described above. At pre-determined times, samples were taken and the dye concentration was determined spectrophotometrically at 430 and 530 nm, for the yellow- and red-dye, respectively.

In order to evaluate the presence of the SDS surfactant as a possible adsorption interferent, the kinetic experiments were also carried-out with the presence of the SDS surfactant, using the proportions dye/SDS of 1:1.

The adsorbed dye quantities were calculated using the expressions [21]:

$$q_t = \frac{(C_i - C_t)V}{m} \quad (1)$$

where q_t is the fixed quantity of dye per gram of Sil-NH_2 at a pre-determined time t in mg g^{-1}, C_i the initial concentration of dye in mg L^{-1}, C_t the concentration of dye present at a pre-determined time t in mg L^{-1}, V the volume of the solution in L and m the mass of Sil-NH_2 in grams.

3. Results and discussion

3.1. Initial considerations

In addition to the specific characteristics of the aminated silica gels cited in Section 1, they are also useful to provide relevant information of the gradual occupation of adsorption sites of the adsorbent material in relation to the variables used in the adsorption works, since only the surface electrostatic interactions are assumed to occur. Other aminated adsorbent materials, mainly organic polymers such as chitosans present gradual opening of the pores at the higher temperatures and lower pH values, which can provoke physical depositions of dyes into the inner parts of the adsorbent [22].

The TG curves of the unmodified and Sil-NH_2 silicas are shown in Fig. 2. The first mass losses steps, from about 25 to 120 °C, are due to the loss of physically adsorbed water on the surfaces [21]. The second mass losses steps, from 120 to about 980 °C, are due to the loss of immobilized aminopropyl groups for the Sil-NH_2. The quantities of mass losses (second stages) are 3.35 and 11.67%, for the unmodified and Sil-NH_2 silicas, respectively. However, since the silica silanization reaction use about 50% of the total content of the silanol groups of the silica [16], the second mass loss stage for Sil-NH_2 is also attributed to the loss of water from the condensation of the residual unreacted silanol groups [16]. From the TG quantitative analysis methodology [16] of the second stage mass loss a quantity of 5.00% (28.5 mg of N g^{-1} of Sil-NH_2) of amine groups (error analysis

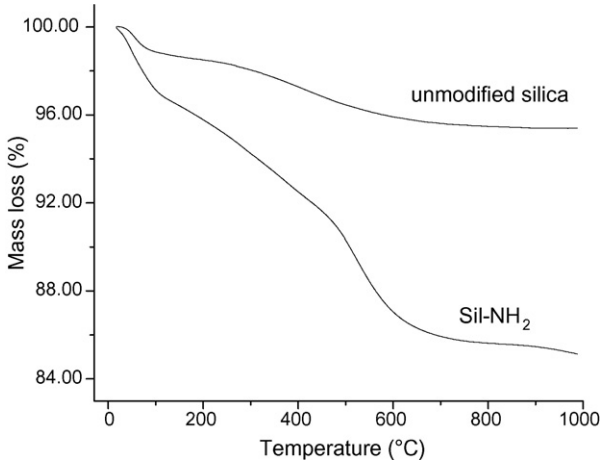

Fig. 2. TG curves of the pure silica and Sil-NH_2.

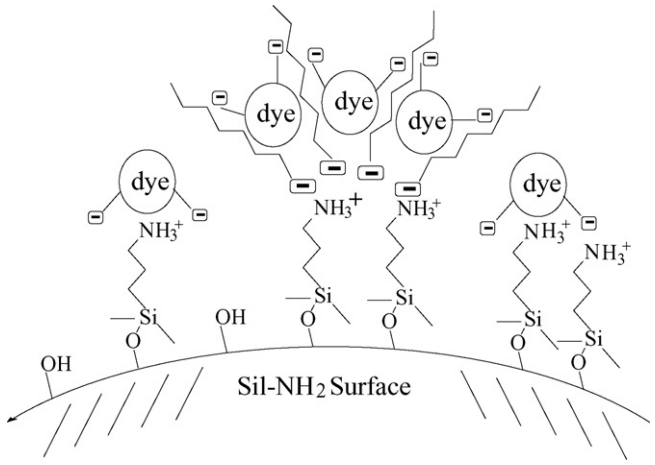

Fig. 3. Schematic representation of the interaction of the anionic dyes with Sil-NH_2 in the presence of an anionic surfactant SDS.

of ±0.15%) was found. The Kjeldhal analysis of the Sil-NH_2 showed the presence of 30.0 mg of N g^{-1} of Sil-NH_2.

The surface area analyses were 300 and 190 m^2 g^{-1} of material, for the unmodified silica and Sil-NH_2, respectively. The decrease of the surface areas reflects the occupation of small pores of the silica by the apts molecules [16,19,20].

Surfactants are used very often to modify the surface properties of various materials, such as their surface charge or hydrophobicity/hydrophilicity. In this way, the sorption of various substances (typically organic compounds) can be supported (coadsorption), or even the sorption of normally non-retained species may be enabled (adsolubilization) [13]. However, a prediction of the effects of surfactants on sorption is not easy, as several simultaneous and competitive mechanisms may be operating during the sorption process. In general, at low SDS concentrations, the dye sorption increased with increasing surfactant concentration. At high SDS concentrations, on the other hand, the dye sorption was suppressed steeply as a result of the complete micelle formation and dye solubilization [23]. The schema of the Fig. 3 represents a general view of the possible interactions that occur with the Sil-NH_2 and the dyes (represented in a simplified manner). Since the experiments were carried out below the cmc of the surfactant, the dyes/SDS aggregates occur partially. So, the interactions of the dyes with the Sil-NH_2 can be represented by the "free dyes" in solution and by the dyes/SDS aggregates, according to references [23,24].

The cmc for each dye/SDS system was determined with the aid of electrical conductivity measurements by plotting the specific conductivities (κ) of dyes solutions as a function of cumulative presence of the SDS in the solutions. Reproducible breaks were observed in each plot indicating the onset of aggregation (Fig. 4). The cmc values obtained were 162.3 ± 1.0 and 123.1 ± 1.0 mg L^{-1}, for the yellow- and red-dye/SDS aggregates, respectively. Blank tests indicated that the cmc of the SDS in the pH 4.0 buffered solutions (without dye in solution) was 73.5 mg L^{-1}. The differences of the cmc values for the SDS/dye and pure SDS have been related to the quantity of interactions of the hydrophobic microdomains of the dyes with the surfactant aggregates [24]. In the present study, the hydrophobic interac-

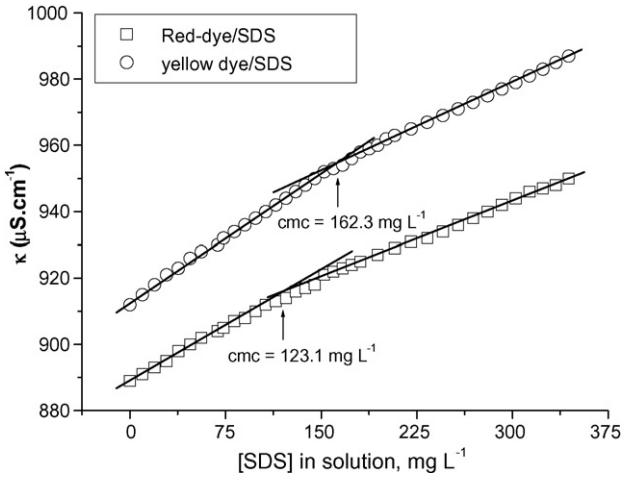

Fig. 4. Specific conductance versus surfactant concentration plots at 25 °C for the yellow- and red-dye.

tions of the system yellow-dye/SDS seem to be higher than the red-dye/SDS due to, probably, the relative small chemical structure of the yellow dye [23]. The lower affinity suggested for the red dye/SDS aggregates may also due to negative charge–charge repulsions of the sulfonate groups of the red-dye chemical structure. On the other hand, the differences of the cmc values for SDS/dye systems not only may be probably due to hydrophobic interactions. A combination of interactions in the hydrophobic region of the mixed micelles and the polar micelle–water interface should also be occurring.

The DSC curves of the Sil-NH_2 silica with the presence of the dyes and dyes/SDS are shown in Fig. 5. The most significant differences in the shape of the curves are observed when the yellow-dye is adsorbed on the Sil-NH_2. The DSC curves seem to indicate the "deep penetration mechanism" (or deeper interaction of the yellow dye into the SDS premicelles) [23]. The DSC curves are very different in nature, indicating the different adsorbed species are present on the Sil-NH_2 surface, before and after the presence of the SDS. The DSC curves for the red-dye interactions are more similar each other, which seem to indicate a lower formation of red-dye/SDS aggregates on the Sil-NH_2 surface.

This behavior seems to confirm the preferential interaction of the SDS with the yellow dye, as observed in the conductometric titration results of this work.

3.2. Kinetic of dyes removal

Figs. 6 and 7 show the dyes adsorption amounts on the Sil-NH_2. It can be seen that the adsorption equilibria are observed after about 160 min of contact time. In general, the presence of the anionic surfactant SDS increased the adsorption quantities. The exception is observed in the yellow-dye adsorption curve at 55 °C. In this case, it seems to be suggested that the yellow-dye/SDS aggregations are not stable at 55 °C. In this form, both anionic yellow dye and the anionic SDS surfactant (probably in its monomeric form at this temperature) compete by the protonated adsorption sites of the Sil-NH_2. So, at 55 °C, the adsorption

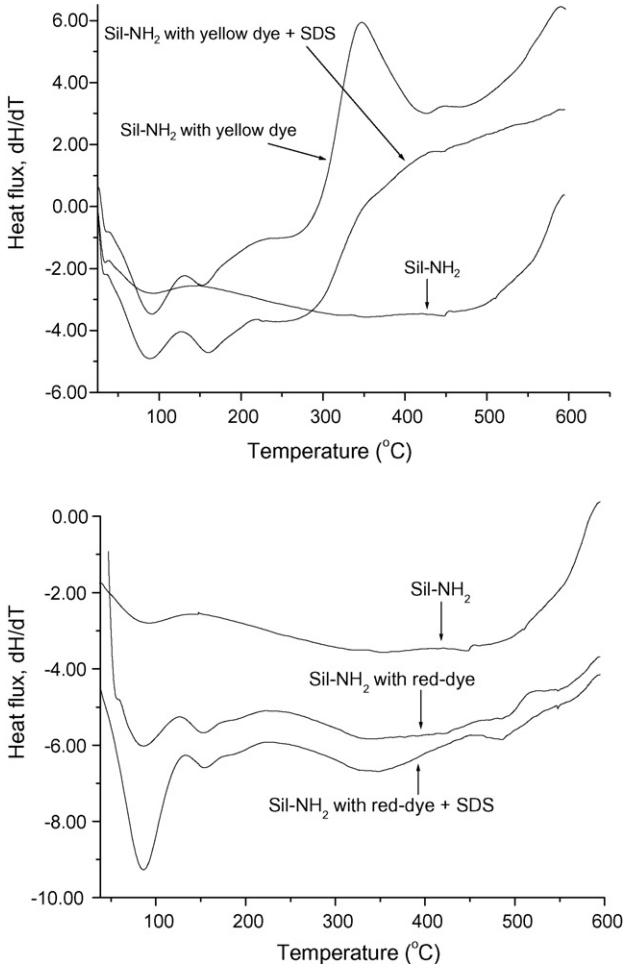

Fig. 5. DSC curves for the interactions of the yellow-dye (upper figure) and red-dye (lower figure) with Sil-NH_2 in the presence of the anionic surfactant SDS.

quantities of the yellow dye decrease in the presence of the SDS. This "competition effect" seems not to be observed, in a significant extension, in the other adsorption experiments in present study, where the presence of the SDS surfactant increased the dyes adsorptions amounts by the formation of premicellar structures (below the cmc of dye/SDS aggregations).

The adsorption behavior of anionic dyes is directly related to some important experimental factors, as pH of solution, the characteristics of the adsorbent, the dimensions of the dye molecular structure, the amount and positioning of the sulfonate groups of the dyes, and the adsorption temperature [25]. The adsorption processes occurs taking into account two main aspects. Firstly, the dye molecules are transferred from the solution to the adsorbent surface. The last stage is related to the diffusion of the dye-adsorbed molecules within the pores of material, binding the pores and capillary spaces. However, both mentioned adsorption processes can present different rates, which are also related to variations of the adsorption temperature.

3.2.1. Modeling of solid-phase adsorption kinetics

Traditionally, the adsorption kinetics of metal ions is described following the expressions originally given by Lager-

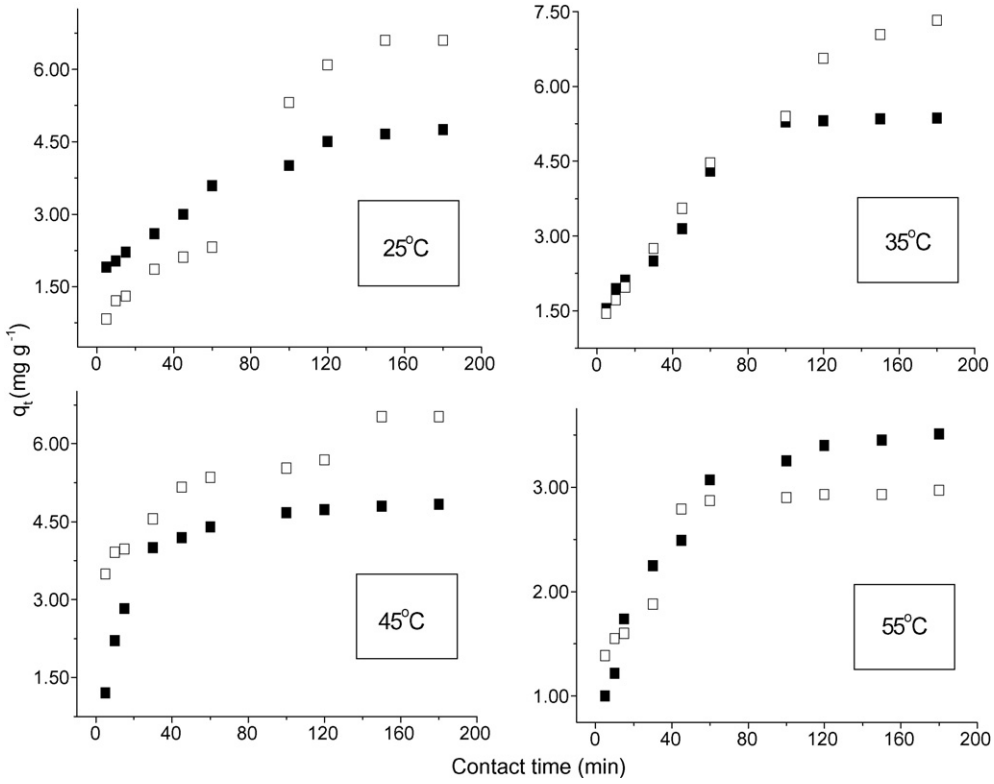

Fig. 6. Profiles of the interaction of the yellow-dye with Sil-NH_2, in relation to the contact time, temperature and the absence (full squares) and the presence (empty squares) of the anionic surfactant SDS.

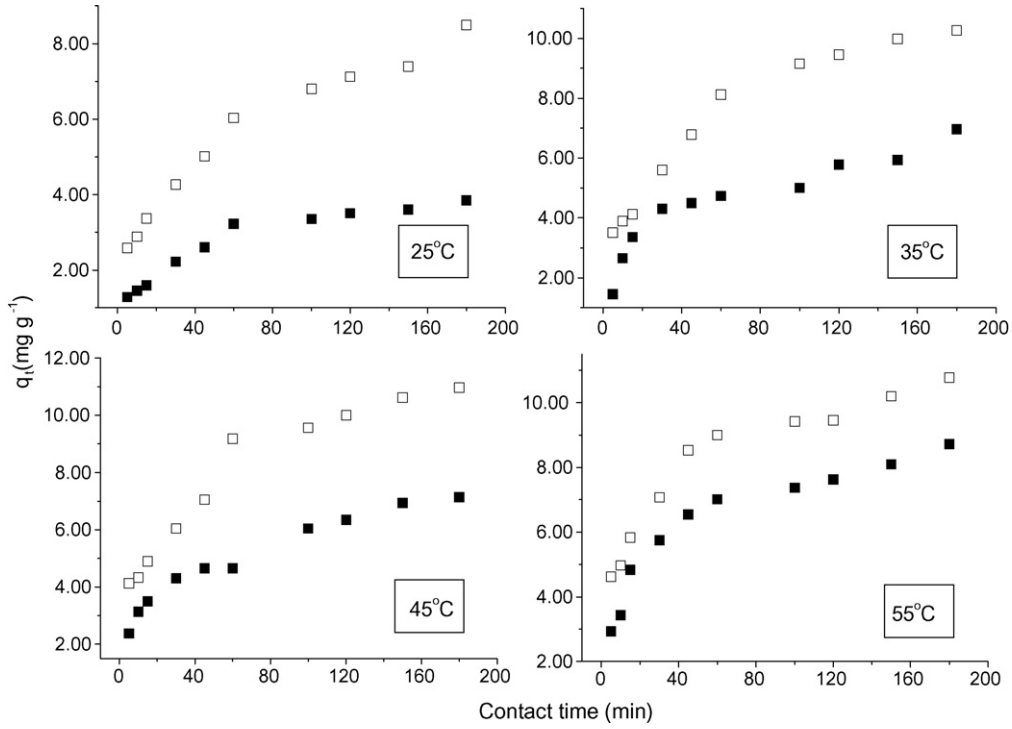

Fig. 7. Profiles of the interaction of the red-dye with Sil-NH_2, in relation to the contact time, temperature and the absence (full squares) and the presence (empty squares) of the anionic surfactant SDS.

gren, which are special cases for the general Langmuir rate equation [25]. A simple kinetic analysis of adsorption is the pseudo-first-order equation in the form:

$$\frac{dq_t}{dt} = k_{1,s}(q_e - q_t) \quad (2)$$

where $k_{1,s}$ is the pseudo-first-order rate constant that relates to the amount of dye adsorbed by the solid phase (Sil-NH_2) and q_e denotes the amount of adsorption at equilibrium. After definite integration and applying the initial conditions $q_t = 0$ at $t = 0$ and $q_t = q_t$ at $t = t$, Eq. (2) becomes:

$$\ln(q_e - q_t) = \ln(q_e) - k_{1,s}t \quad (3)$$

In addition, a pseudo-second-order equation based on adsorption equilibrium capacity may be expressed in the form:

$$\frac{dq_t}{dt} = k_{2,s}(q_e - q_t)^2 \quad (4)$$

where $k_{2,s}$ is the pseudo-second-order rate constant that relates to the amount of dye adsorbed by the solid phase (Sil-NH_2). Integrating Eq. (3) and applying the initial conditions, we have:

$$\frac{1}{q_e - q_t} = \frac{1}{q_e} + k_{2,s}t \quad (5)$$

or equivalently:

$$\frac{t}{q_t} = \frac{1}{k_{2,s}q_e^2} + \frac{1}{q_e}t \quad (6)$$

It should be noted that, compared to Eq. (4), Eq. (5) has an advantage that $k_{2,s}$ and q_e can be obtained from the intercept and slope of the plot of (t/q_t) versus t and there is no need to know the q_e parameter (at equilibrium) beforehand [25].

The fitting validity of these models is traditionally checked by the linear plots (plots not shown) of $\ln(q_e - q_t)$ versus t, and (t/q_t) versus t, respectively. From the slope and intersection of the straight line obtained, the corresponding constant values for the pseudo-first- and pseudo-second-order kinetic models, for each temperature studied, provides the respective kinetic constants, $k_{i,s}$ ($i = 1$ or 2), and the q_e parameters.

Despite the Lagergren kinetic equations has been used for the most adsorption kinetic works, determination of some specific kinetic parameters, as possible changes of the adsorption rates in function of the contact time and temperature represent still lacks and a challenge in the kinetic adsorption modelings. In this way, an alternative Avrami kinetic equation is also used in this work. The adsorption should also be visualized using the Avrami exponential function shown in Eq. (7), which was successful used earlier in adsorption studies of Hg^{2+} on thin chitosan membranes [26], silica-dithizone [27] and recently, in adsorption of reactive dyes on silica/chitosan hybrid [28]:

$$q_t = q_e\left(1 - \exp^{-[k_{Av}t]^n}\right) \quad (7)$$

where k_{Av} is the Avrami kinetic constant and n is another constant, which is related to the adsorption mechanisms changes. The linearized form of this equation is presented in Eq. (8):

$$\ln\left(\ln\left(\frac{q_e}{q_e - q_t}\right)\right) = n\ln k_{Av} + n\ln t \quad (8)$$

The $\ln(\ln(q_e/q_e - q_t))$ versus $\ln t$ plots (plots not shown) in relation to adsorption temperature provide the n and $\ln k_{Av}$ values from the slopes and intersections values, respectively. In general, the contact time ranges for the multi-linearized Avrami plots were 5–15, 15–60, 60–100 and 100–180 min. So, the formation of three or four linear regions, in relation to the temperature and the contact time, is strongly suggested and independent values of $n_{i(i=1–4)}$ and $k_{Av,i(i=1–4)}$ should also be considered. The calculated n and k_{Av} Avrami constants are different from 25 to 55 °C. In this manner, for this temperature range, the adsorptions of the dyes seem to present both temperature and contact time depen-

Table 1
Lagergren second-order and Avrami kinetic parameters related to the interactions of the yellow- and red-dye into the Sil-NH_2 in absence (upper half) and presence (lower half) of the surfactant SDS

Dye	Temperature (°C)	k_2 ($\times 10^{-3}$ min^{-1})	Q_e (mg g^{-1})	$k_{Av,1}$ ($\times 10^{-3}$ min^{-1})	n_1	$k_{Av,2}$ ($\times 10^{-2}$ min^{-1})	n_2	$k_{Av,3}$ ($\times 10^{-2}$ min^{-1})	n_3	$k_{Av,4}$ ($\times 10^{-2}$ min^{-1})	n_4
Yellow	25	8.72	5.22	12.5	0.25	22.5	0.69	1.51	1.70	–	–
	35	6.24	6.09	4.39	0.41	2.23	1.52	22.6	0.46	1.16	2.97
	45	17.0	5.17	60.2	1.02	109.0	0.45	3.41	0.97	–	
	55	14.3	3.83	33.3	0.63	2.49	1.80	8.71	0.44	2.13	1.28
Red	25	8.17	4.24	13.2	0.35	1.92	0.88	–	–	–	–
	35	3.37	7.69	4.49	0.95	1.74	0.28	1.11	1.05	–	–
	45	3.73	7.95	24.7	0.41	1.45	0.18	1.67	0.87	0.89	2.69
	55	3.12	9.47	1.16	0.17	1.90	0.61	–	–	–	
Yellow	25	0.79	9.24	1.87	0.46	1.03	1.74	–	–	–	–
	35	1.88	7.54	4.39	0.41	1.37	0.87	1.18	1.79	–	–
	45	11.6	3.40	55.1	0.19	5.13	0.49	0.33	0.17	1.28	1.43
	55	32.5	1.70	29.8	0.25	3.50	1.80	8.29	0.19	5.03	0.81
Red	25	2.29	9.82	3.49	0.26	1.31	0.70	1.86	0.51	0.66	4.04
	35	2.73	11.52	7.99	0.15	1.73	0.94	3.26	0.58	1.05	2.04
	45	2.78	12.11	8.73	0.25	1.75	0.90	0.60	1.06	–	–
	55	2.88	11.63	5.58	0.19	1.77	0.76	–	–	–	–

Table 2
Comparative fitting data of the second-order Lagergren and Avrami model

Dye	Temperature (°C)	With SDS, Δq_t (%)		Without SDS, Δq_t (%)	
		Lagergren (second-order)	Avrami	Lagergren (second-order)	Avrami
Yellow	25	6.63	5.19	19.65	3.04
	35	19.48	3.90	18.66	11.54
	45	17.75	2.47	10.49	1.15
	55	13.54	0.25	8.04	4.61
Red	25	24.32	2.38	21.47	2.68
	35	24.91	12.41	20.36	4.38
	45	21.85	3.01	23.71	7.53
	55	23.93	10.91	20.97	11.63

dence in relation to the adsorption kinetic parameters. Table 1 shows the numerical values of the models parameters. In general, the kinetic constants ($k_{Av,i}$) decrease when the contact time increases. From both the Table 1 results and the literature considerations [3,25], the first stages (n_1 and $k_{Av,1}$) for both dyes, in the absence and in the presence of SDS are relatively slow and they are related to (mainly) the occupation of the surface adsorption sites. The other stages are relatively fast and they are associated with the diffusional interaction of dyes into the adsorption sites present in the pores of the adsorbent. However, the extension of the diffusion is a function of the temperature and the type of dye. For the yellow dye, in the absence and the presence of SDS, the increasing of temperature seems to stimulate the diffusion processes into the adsorption sites on the pores. However, the presence of SDS seems to be stimulated the diffusion of the red-dye into the adsorption sites.

In order to quantitatively compare the applicability of each solid-phase kinetic model, the Table 2 shows the normalized standard deviations (Δq_t), which are obtained as follows [29]:

$$\Delta q_t\,(\%) = 100 \times \sqrt{\frac{\sum[(q_{t,\mathrm{exp}} - q_{t,\mathrm{calc}})/q_{t,\mathrm{exp}}]^2}{a-1}} \qquad (9)$$

where $q_{t,\mathrm{calc}}$ are the adsorption calculated values from both the Lagergren and the Avrami models and a is the number of experimental points of the kinetic curves. From inspections of the Table 2, good agreements of the experimental and calculated data were found using the Avrami model for all contact time evaluated ($12.00 \leq \Delta q_t\ (\%) \leq 0.25$). Good linear fittings were also detected using the pseudo-second-order kinetic model (r^2-values at least of 0.9880). However, the experimental-calculated confrontations produced poorer fittings in relation to the Lagergren kinetic data, as observed in Table 2 ($24.90 \leq \Delta q_t\ (\%) \leq 6.60$).

4. Conclusions

In this study, the aminopropyl-silica (Sil-NH_2) was used to adsorb a yellow- and a red-dye from aqueous solutions at pH 4.0. New data concerning the influence of the anionic surfactant SDS on the adsorption data was obtained. All interactions occurred

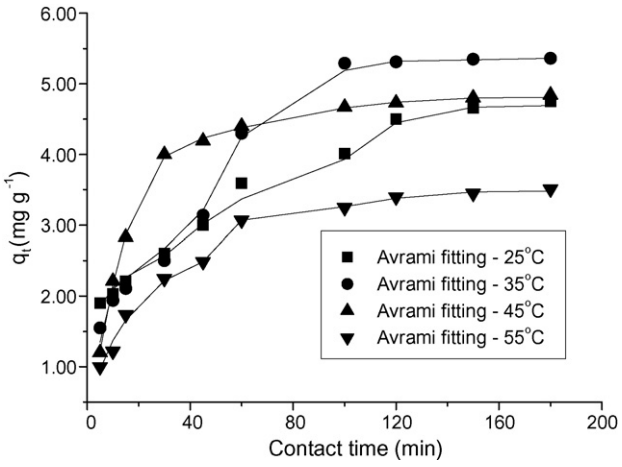

Fig. 8. Comparison of the Avrami model fitting to the yellow-dye adsorption experimental data in the absence of SDS at different temperatures. Experimental data are reported as points and the Avrami calculated data as curves.

below the cmc values of the Sil-NH_2/anionic dyes aggregates. A rise of temperature accelerates the mass transfer of the red-dye into the Sil-NH_2 surface, while the yellow-dye adsorption decreased.

The presence of SDS increased the adsorption quantities in relation to the temperature increasing. The exception is observed for the yellow-dye adsorption at 55 °C. So, it is suggested that the chemical structure of this dye, as well as the presence and position of its sulfonate groups are important factors that affect the cmc of the anionic dye/SDS aggregations and the adsorption quantities.

The solid-phase interactions of dyes data present a good fitting to the Avrami kinetic model (Figs. 8–11). From this model, from two to four kinetic regions were found, taking into account the variations of the contact time and temperature. The variations of the Avrami constants, namely $n_{i(i=1–4)}$ and $k_{Av,i(i=1–4)}$, have been attributed to the occupation of both the surface and the internal adsorption sites of the aminopropyl-silica.

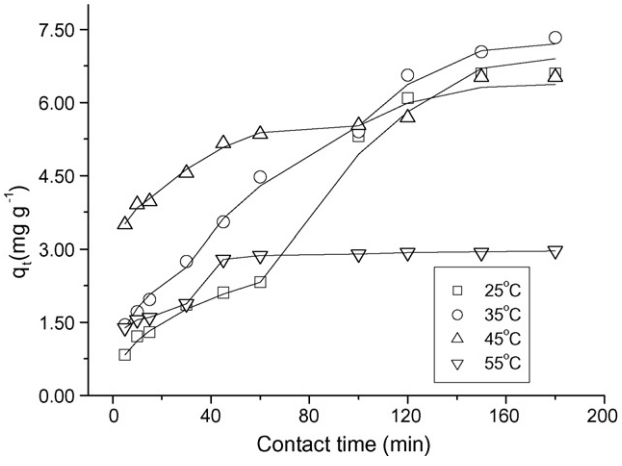

Fig. 9. Comparison of the Avrami model fitting to the red-dye adsorption experimental data in the absence of SDS at different temperatures. Experimental data are reported as points and the Avrami calculated data as curves.

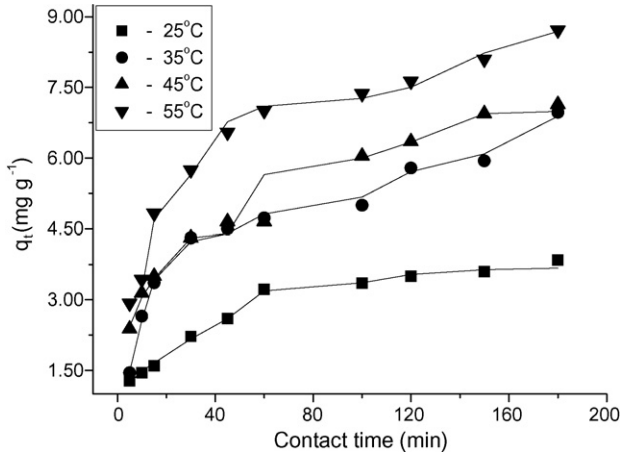

Fig. 10. Comparison of the Avrami model fitting to the yellow-dye adsorption experimental data in the presence of SDS at different temperatures. Experimental data are reported as points and the Avrami calculated data as curves.

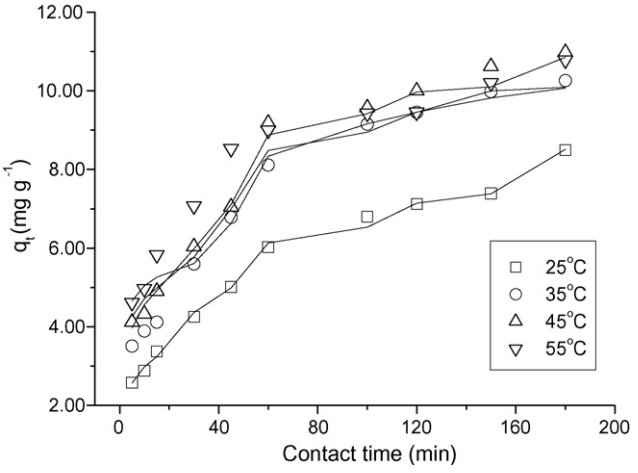

Fig. 11. Comparison of the Avrami model fitting to the red-dye adsorption experimental data in the presence of SDS at different temperatures. Experimental data are reported as points and the Avrami calculated data as curves.

Acknowledgments

The authors thank the Brazilian National Agency CNPq for fellowships to G.S.V. and A.R.C., The Santista Textiles Company (Sergipe/Brazil) for the free-gift dyes samples and The Dystar Dyes Company (Brazilian office), for the essential dyes technical information to our research group.

References

[1] B. Nigam, G. Armour, I.M. Banat, D. Singh, R. Marchant, Physical removal of textile dyes from effluents and solid-state fermentation of dye-adsorbed agricultural residues, Bioresour. Technol. 72 (2000) 219–226.

[2] G. Crini, Recent developments in polysaccharide-based materials used as adsorbents in wastewater treatment, Prog. Polym. Sci. 30 (2005) 38–70.

[3] Y.S. Ho, Selection of optimum sorption isotherm, Carbon 42 (2004) 2113–2130.

[4] Indian Standards Institution, Methods of Sampling and Tests for Activated Carbon Used for Decolourising Vegetable Oils and Sugar Solutions, Indian Standards Institution, 1977 (IS 877).

[5] U. Ciesla, F. Schüth, Ordered mesoporous materials, Micropor. Mesopor. Mater. 27 (1999) 131–149.

[6] M.A. Hassanien, K.S. Abou-El-Sherbini, Synthesis and characterization of morin-functionalized silica gel for the enrichment of some precious metal ions, Talanta 68 (2006) 1550–1559.

[7] M. Sliwka-Kaszynska, K. Jaszczolt, A. Kolodziejczyk, J. Rachon, 1,3-alternate 25,27-dibenzoiloxy-26,28-bis-[3-propyloxy]-calix[4]arene-bonded silica gel as a new type of HPLC stationary phase, Talanta 68 (2006) 1560–1566.

[8] M. Mifune, K. Kawata, K. Tanaka, Y. Kitamura, I. Tsukamoto, M. Saito, J. Haginaka, Y. Saito, HPLC retention behaviors of poly-aromatic-hydrocarbons on Cu(II)-octabromotetrakis(4-carboxyphenyl)porphine derivatives-immobilized aminopropyl silica gels in polar and non-polar eluents, Chem. Pharm. Bull. 54 (2006) 94–98.

[9] P.G. Zanichelli, R.L. Sernaglia, D.W. Franco, Immobilization of the [Ru-II(edta)NO+] ion on the surface of functionalized silica gel, Langmuir 22 (2006) 203–208.

[10] J.C. Valette, C. Demesmay, J.L. Rocca, E. Verdon, Potential use of an aminopropyl stationary phase in hydrophilic interaction capillary electrochromatography. Application to tetracycline antibiotics, Chromatographia 62 (2005) 393–399.

[11] T. Jesionowski, S. Binkowski, A. Krysztafkiewicz, Adsorption of the selected organic dyes on the functionalized surface of precipitated silica via emulsion route, Dyes Pigments 65 (2005) 267–279.

[12] A. Andrzejewska, A. Krysztafkiewicz, T. Jesionowski, Adsorption of organic dyes on the aminosilane modified TiO_2 surface, Dyes Pigments 62 (2004) 121–130.

[13] P. Janoš, V. Šmídová, Effects of surfactants on the adsorptive removal of basic dyes from water using an organomineral sorbent—iron humate, J. Colloid Interf. Sci. 291 (2005) 19–27.

[14] L.F.C. Melo, C.H. Collins, I.C.S.F. Jardim, High-performance liquid chromatographic determination of pesticides in tomatoes using laboratory-made NH_2 and C-18 solid-phase extraction materials, J. Chromatogr. 1073 (2005) 75–81.

[15] O. Leal, C. Bolévar, C. Ovalles, J.J. Garcia, Y. Espidel, Reversible adsorption of carbon dioxide on amine surface-bonded silica gel, Inorg. Chim. Acta 240 (1995) 183–189.

[16] A.R. Cestari, C. Airoldi, A new elemental analysis method based on thermogravimetric data and applied to alkoxysilane immobilized on silicas, J. Therm. Anal. 44 (1995) 79–85.

[17] A.R. Cestari, E.F.S. Vieira, R.E. Bruns, C. Airoldi, Some new data for metal desorption on inorganic–organic hybrid materials, J. Colloid Interf. Sci. 227 (2000) 66–70.

[18] S. Bhattacharya, J. Haldar, Microcalorimetric and conductivity studies with micelles prepared from multi-headed pyridinium surfactants, Langmuir 21 (2005) 5747–5751.

[19] A.R. Cestari, E.F.S. Vieira, E.S. Silva, Interactions of anionic dyes with silica-aminopropyl. I. A quantitative multivariate analysis of equilibrium adsorption and adsorption Gibbs free energies, J. Colloid Interf. Sci., in press.

[20] E.F.S. Vieira, A.R. Cestari, J.A. Simoni, C. Airoldi, Thermochemical data for interaction of some primary amines with complexed mercury on mercapto-modified silica gel, Thermochim. Acta 399 (2003) 121–126.

[21] A.R. Cestari, E.F.S. Vieira, A.G.P. Santos, J.A. Mota, V.P. Almeida, Adsorption of anionic dyes on chitosan beads. Part I. The influence of the chemical structures of dyes and temperature on the kinetics of adsorption, J. Colloid Interf. Sci. 280 (2004) 380–386.

[22] E. Guibal, Heterogeneous catalysis on chitosan-based materials: a review, Prog. Polym. Sci. 30 (2005) 71–109.

[23] J. Oakes, P. Gratton, Solubilization of dyes by surfactant micelles. Part 1. Molecular interactions of azo dyes with non-ionic and anionic surfactants, Color Technol. 119 (2003) 91–99.

[24] P. Relógio, J.M.G. Martinho, J.P.S. Farinha, Effect of surfactant on the intra- and intermolecular association of hydrophobically modified poly(*N*,*N*-dimethylacrylamide), Macromolecules 38 (2005) 10799–10811.

[25] Y.S. Ho, G. McKay, Sorption of dyes and copper ions onto biosorbents, Process Biochem. 38 (2003) 1047–1061.

[26] E.C.N. Lopes, F.S.C. dos Anjos, E.F.S. Vieira, A.R. Cestari, An alternative Avrami equation to evaluate kinetic parameters of the interaction of Hg(II) with thin chitosan membranes, J. Colloid Interf. Sci. 263 (2003) 542–547.

[27] A.R. Cestari, E.F.S. Vieira, E.C.N. Lopes, R.G. da Silva, Kinetics and equilibrium parameters of Hg(II) adsorption on silica-dithizone, J. Colloid Interf. Sci. 272 (2004) 271–276.

[28] A.R. Cestari, E.F.S. Vieira, A.A. Pinto, E.C.N. Lopes, Multi-steps adsorption of anionic dyes on silica/chitosan hybrid. I. Comparative kinetic data from liquid- and solid-phase models, J. Colloid Interf. Sci. 292 (2005) 363–372.

[29] F.C. Wu, R.L. Tseng, R.S. Juang, Preparation of highly microporous carbons from fir wood by KOH activation for adsorption of dyes and phenols from water, Separ. Purif. Technol. 47 (2005) 10–19.